Supplementary Information

Harnessing of the Nucleosome Remodeling Deacetylase complex controls lymphocyte development and prevents leukemogenesis

Jiangwen Zhang[1*], Audrey F. Jackson[2*], Taku Naito[2,3*], Marei Dose[4], John Seavitt[2], Feifei Liu[2], Elizabeth J. Heller[2], Mariko Kashiwagi[2], Toshimi Yoshida[2], Fotini Gounari[4], Howard T. Petrie[5] and Katia Georgopoulos[2]

Correspondence: email: katia.georgopoulos@cbrc2.mgh.harvard.edu

Supplementary Methods

Mononucleosome DNase I Disruption Assay

A 155bp of DNA fragment (EcoRI-Mlu I) from the TPT plasmid[1] with two copies of a 20-bp artificial nucleosome positioning sequence, a TATA box and engineered to contain Ikaros sites (Ik+) or their mutated counterparts (Ik-) was ^{32}P-labeled at the 5' end and assembled into a mononucleosomal core particle in the presence of purified HeLa core histones by salt dilution as described[2]. Assembled templates were purified by glycerol gradient sedimentation and 3.3 ng of nucleosome core particles was incubated with or without ATP and Ikaros-NuRD complex in the reaction. Reactions were incubated at 30°C for 30 min, treated with DNase I for 2 min at room temperature (0.2 units for mononucleosomes or 0.02 units for naked DNA), and analyzed on an 8% SDS-PAGE denaturing gel. Electrophoretic mobility assays with naked DNA or nucleosomes were performed on 4% native acrylamide gels as previously described[3]

5S array restriction enzyme accessibility assay.

Restriction enzyme accessibility assays were performed with 5S arrays as previously described[4]. The Gal4 DNA binding sites of the p2085S-G5E4 plasmid normally used in this assay [4] were replaced with 7 Ikaros sites (Ik+). The 5S-Ik+ fragment was excised from the plasmid and purified over a Sephacryl™ S-1000 Superfine column (Amersham Pharmacia Biotech AB), end labeled and assembled into a polynucleosomal template by gradient dialysis as described previously[5]. 0.3 U/µl of Hha I were used in

the reaction which included the Ikaros-NuRD or the hSWI/SNF complex. Aliquots were removed to a deproteinating stop buffer at 0, 2, 10, 40, and 60 min and allowed to incubate at 30°C for 30 min. The samples were loaded on a 1% agarose gel in 1X TBE and analyzed by phosphoimager for quantification. Competition reactions were performed with 50-100ng of cold Ikaros binding or non-binding oligonucleotides.

Supplementary Figure Legends

Supplementary Figure 1. Hierarchical clustering confirms extensive overlap between Ikaros and Mi–2β at the chromatin level. Ward's hierarchical clustering of normalized ChIP-Seq signal for Ikaros (**a**) or Mi–2β (**b**) in WT chromatin reveals extensive overlap between the two factors at the binding site level (**d)**, Heat map of Mi–2β binding signal in WT and ΔIk chromatin from –1 kb to +1 kb surrounding the center of all the Mi–2β binding sites, ordered by strength of Mi–2β binding in ΔIk chromatin.

Supplementary Figure 2. Western blot analysis of Mi-2β protein in WT, ΔIk, ΔNotch1(N1), and ΔIkΔN1 thymocyte extracts. The expression of Notch1 and Ikaros proteins are shown as controls.

Supplementary Figure 3. Ikaros DNA binding effects on nucleosome remodeling. Binding of the Ikaros-NuRD complex (Ik-c, 50ng) to naked DNA templates **(a)** or DNA incorporated into mononucleosomes **(b)** with (+) or without (-) Ikaros binding sites. Reactions were also performed in the presence of Ikaros monoclonal antibodies (αIk) or ATP. Presence of ATP stimulated binding of the Ikaros complex to nucleosomal templates

bearing Ikaros binding sites. Incubations were performed for 30 min at 30^0C and analyzed on a 4% native acrylamide gel. (**c**) Mononucleosome disruption by the Ikaros-NuRD (88 and 11 ng) complex or Aiolos-NuRD (11ng) complex in the presence of ATP visualized by changes in the 10bp DNase I digestion pattern of core nucleosomes. The first lane in each set indicates DNAse I digestion of naked DNA (N). Blue stars indicate ATP-specific changes seen preferentially on nucleosomal templates without Ikaros sites. (**d**) Effect of Ikaros binding and non-binding oligos (50, 100 ng) to enzyme accessibility reaction measured by Hha I digestion in the presence of Ikaros-NuRD complex with (squares) or without (circles) ATP. Reactions with 75nM of Ikaros-NuRD complex and Hha I (0.3 units/μλ) were performed for 60min. As a control hSWI/SNF (75nM) purified from HeLa cells that does not contain Ikaros proteins was used.

Supplementary Figure 4. **Heatmap for GO pathway analysis of Mi-2β gene targets with or without Ikaros (Ik+ or Ik-)**. Four categories (vertical lines 1-4) are highlighted with the top GO pathways shown in each category. Category 1 specifically identifies Mi-2β plus Ikaros (+Ik) gene targets, and is enriched in T cell differentiation pathways, category 4 specifically identifies Mi-2β minus Ikaros (-Ik) gene targets, and is enriched in metabolic pathways. Category 2 is highly enriched by Mi-2β (+Ik) and weakly enriched by Mi-2β (-Ik) gene targets whereas category 3 is the opposite.

Supplementary Figure 5. Analysis of H3 modifications in the vicinity of the TSS of down-(a) and up-(b) regulated genes in ΔIk thymocytes. RNA pII and Mi−2β occupancy is also shown. **c**, TSS analysis for H3K4 and H3K9/K14 Ac for down-regulated genes that

were further subdivided into subsets with (w) Mi-2β and without (w/o) Mi-2β. Arrows indicate increase in nucleosome remodeling observed in the vicinity of Mi−2β and lines the further reduction in H3K9/K14Ac at TSS with Mi−2β.

Supplementary Figure 6. Examples of down- and up-regulated genes shown by Integrated genome viewer presentation of Ikaros, Aiolos and Mi-2β sites normalized to WT or ΔIk input controls. Differential analysis of enrichment for Mi-2β, RNA pII and H3 modifications (H3K9/K14Ac, RNA pII, H3K27me3 and H3K36me3) in WT and ΔIk chromatin is also shown. In this comparative analysis (wt vs. ΔIk or ΔIk vs. wt), the presence of reads indicates a signal increase.

Supplementary Figure 7. **Antagonistic effects of NuRD gain of function on lymphocyte differentiation vs. homeostasis.** GO analysis of down- and up-regulated genes grouped into Mi-2β targets with Ikaros or Aiolos (Mi-2βGT ΔIk+Ik/Aio) or Mi-2β alone (Mi-2βGTΔIk-Ik/Aio). The significance in GO enrichment is shown as –log10 (P-value).

Supplementary Figure 8. Differential targeting and bimodal regulation by the Mi-2β/NuRD complex. Targeting of Mi-2β to permissive chromatin is restricted to lymphoid genes by the presence of Ikaros proteins. Here, Mi-2β chromatin access is limited by Ikaros DNA binding, providing a barrier that controls the interplay between HDACs and HATs, loaded concomitantly at active promoters[3]. Reduction in Ikaros DNA binding allows more Mi-2β access to chromatin, increased nucleosome remodeling and histone deacetylation and decreased RNA polII recruitment and lymphoid gene expression. The Mi-2β/NuRD

complex is also re-distributed to the permissive chromatin of transcriptionally poised cell growth and proliferation genes causing their activation, by interfering with PRC2 activity and other repressive mechanisms.

Supplementary Figure 9. Examples of tracks for factor or H3 ChIP-seq experiments and their corresponding input controls after read number normalization are shown for the CD4 locus prior to and after peak enrichment calculation by MACS as described in materials and methods.

Supplementary Table 1.

Protein composition of Mi−2β-flag and flag-Ikaros-based complexes purified from thymocytes of mice transgenic for either an Ikaros-Mi−2β -flag or a CD2- flag-Ikaros expression cassette [3, 6]. A summary of results provided from mass spectrometry and Western blotting (IB) is shown together with the approximate size of the identified proteins. The SMC3 protein component of the cohesin complex was identified by mass spectrometry in the Mi−2β-flag complex. Its presence at low levels (together with other cohesin complex components) was confirmed in both the Mi−2β−NURD but also in the Ikaros-NURD complex by immunoblotting. ND-not determined

Supplementary Table 2.

Genome-wide H3K9/K14Ac, RNA pII and H3K36me3 changes and association with Ikaros, Aiolos or Mi-2β gene targets (GT) established in WT or ΔIk chromatin. Changes in H3 modifications were determined at a P-value of $<10^{-5}$ and at >5 fold change.

Supplementary Table 3. Changes in H3 modifications and Ikaros/Aiolos or Mi-2β occupancy in the up- and down-regulated gene signature defined by combined change in H3K36me3 and RNA expression in Ikaros deficient pre-leukemic thymocytes. The % of genes with loss in H3 modification was calculated at a P-value $<10^{-5}$ and at >2 fold change.

Supplementary References

1. Aalfs, J.D., Narlikar, G.J. & Kingston, R.E. Functional differences between the human ATP-dependent nucleosome remodeling proteins BRG1 and SNF2H. *J Biol Chem* **276**, 34270-34278 (2001).
2. Imbalzano, A.N., Kwon, H., Green, M.R. & Kingston, R.E. Facilitated binding of TATA-binding protein to nucleosomal DNA. *Nature* **370**, 481-485 (1994).
3. Kim, J. *et al.* Ikaros DNA-binding proteins direct formation of chromatin remodeling complexes in lymphocytes. *Immunity* **10**, 345-355 (1999).
4. Neely, K.E. *et al.* Activation domain-mediated targeting of the SWI/SNF complex to promoters stimulates transcription from nucleosome arrays. *Mol Cell* **4**, 649-655 (1999).
5. Luger, K., Rechsteiner, T.J. & Richmond, T.J. Preparation of nucleosome core particle from recombinant histones. *Methods Enzymol* **304**, 3-19 (1999).
6. Kaufmann, C. *et al.* A complex network of regulatory elements in Ikaros and their activity during hemo-lymphopoiesis. *EMBO J* **22**, 2211-2223 (2003).

Supplementary Figure 1

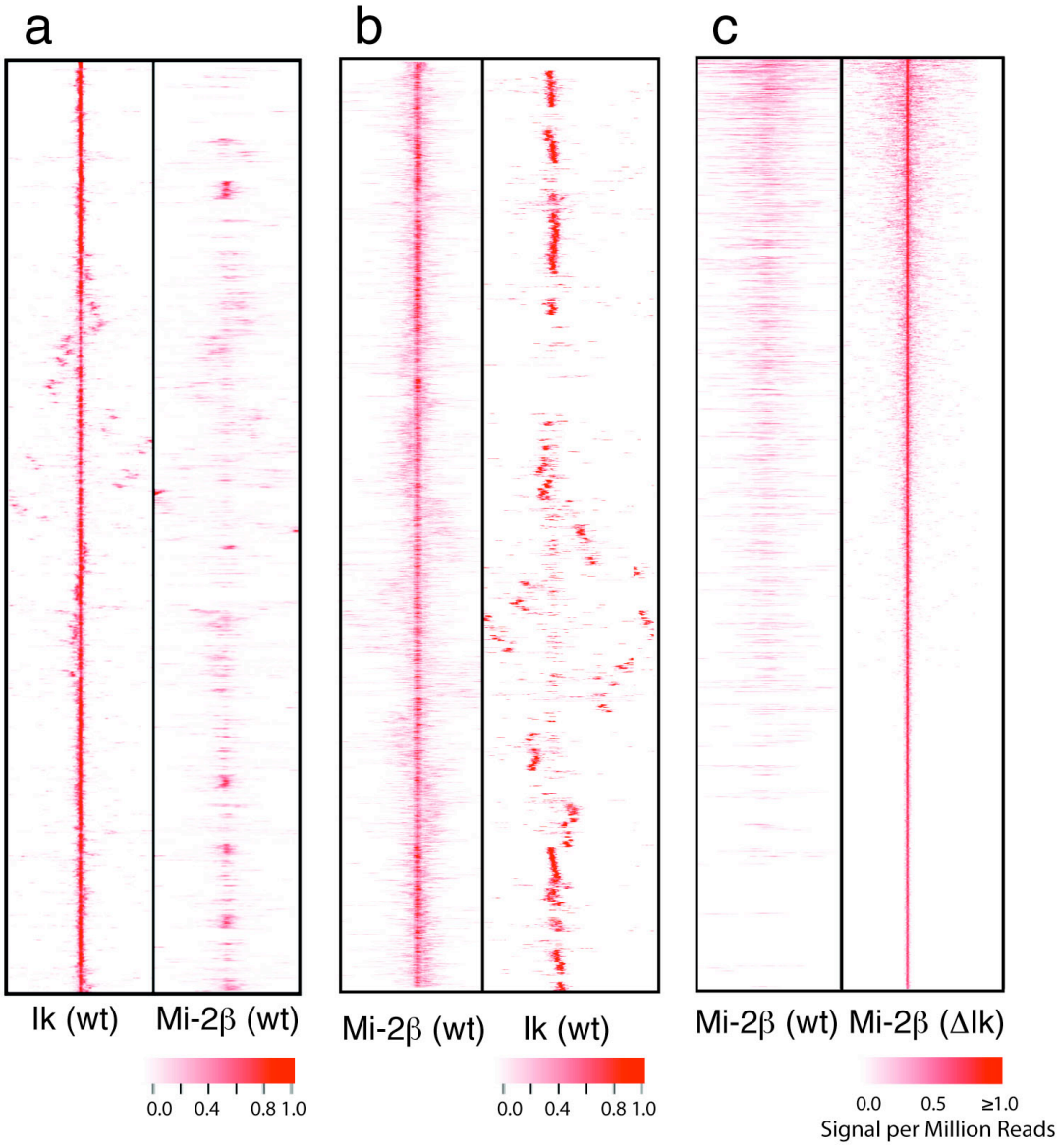

Supplementary Figure 2

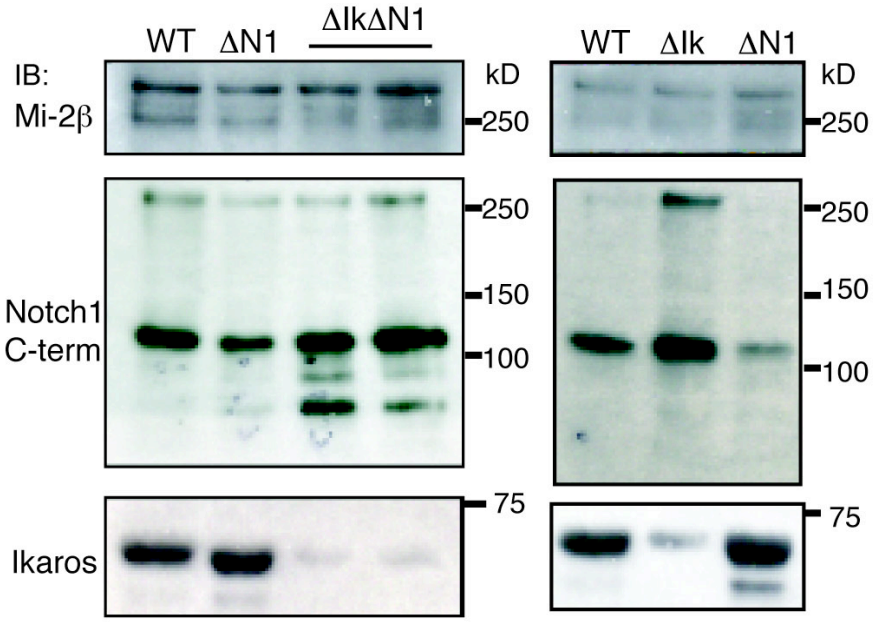

Supplementary Figure 3

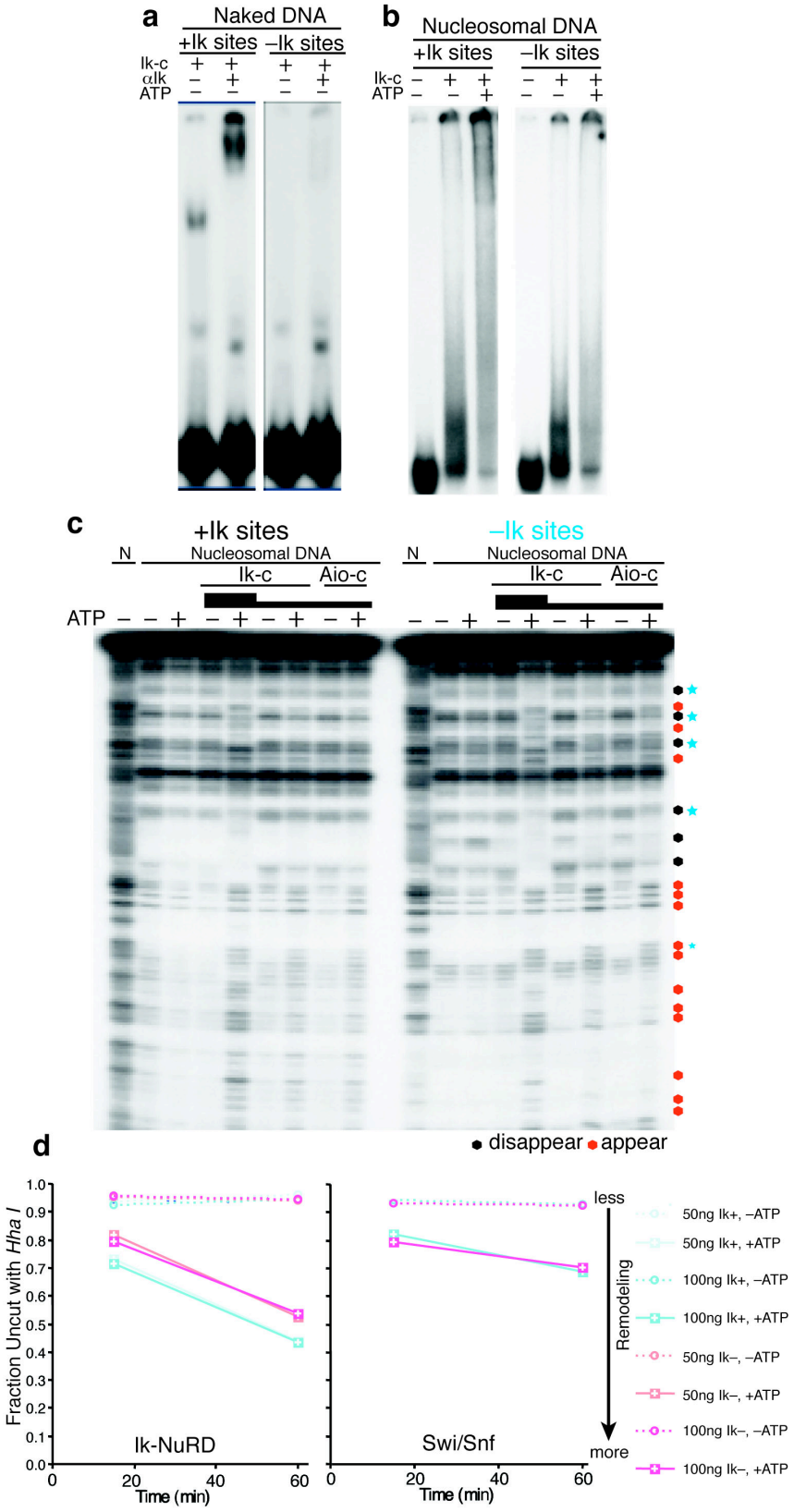

Supplementary Figure 4

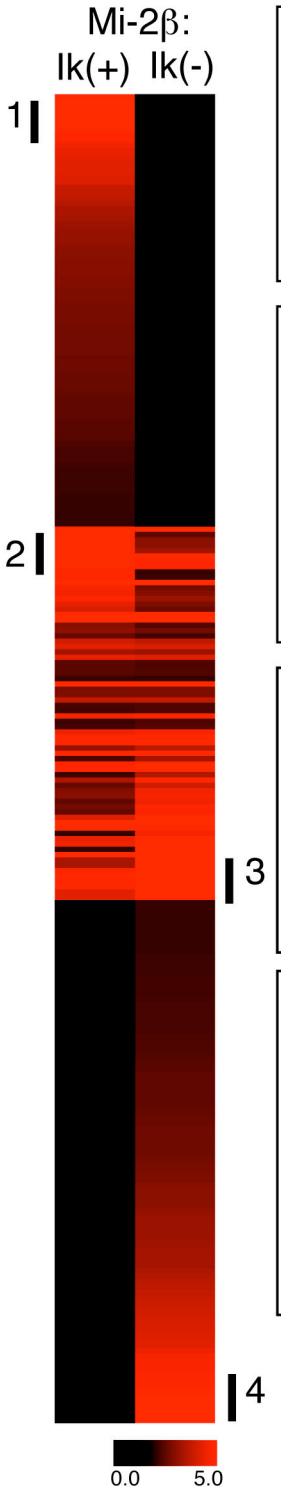

1
- **T cell activation**
- **T cell differentiation**
- DNA repair
- protein aminoacid acylation
- regulation of transcription
- negative regulation of cell-matrix adhesion
- intracellular protein transport
- regulation of phosphorylation

2
- regulation of transcription
- DNA metabolic process
- intracellular transport
- response to DNA damage
- chromatin modification
- **lymphoid organ development**
- **hemopoiesis**
- **immune system development**
- **regulation of cell cycle**
- **regulation of apoptosis**

3
- **positive regulation of apoptosis**
- small GTPAse signal transduction
- chromatin organization
- mRNA processing
- itracellular signaling
- **cell cycle**
- **protein catabolic process**
- **phosphate metabolic process**

4
- ncRNA metabolic process
- mRNA metabolic process
- glycerophospholipid metabolic process
- lipid biosynthetic porcess
- organophosphate metabolic process
- macromolecular complex subunit organization
- regulation of ras protein signal transduction
- **ubiquitin-dependent catabolic process**
- **induction of apoptosis**
- **cell cycle**

Pathways in:
- **T cell differentiation**
- **cell cycle**
- **apoptosis**
- **protein catabolism**
- **cell metabolism**

Supplementary Figure 5

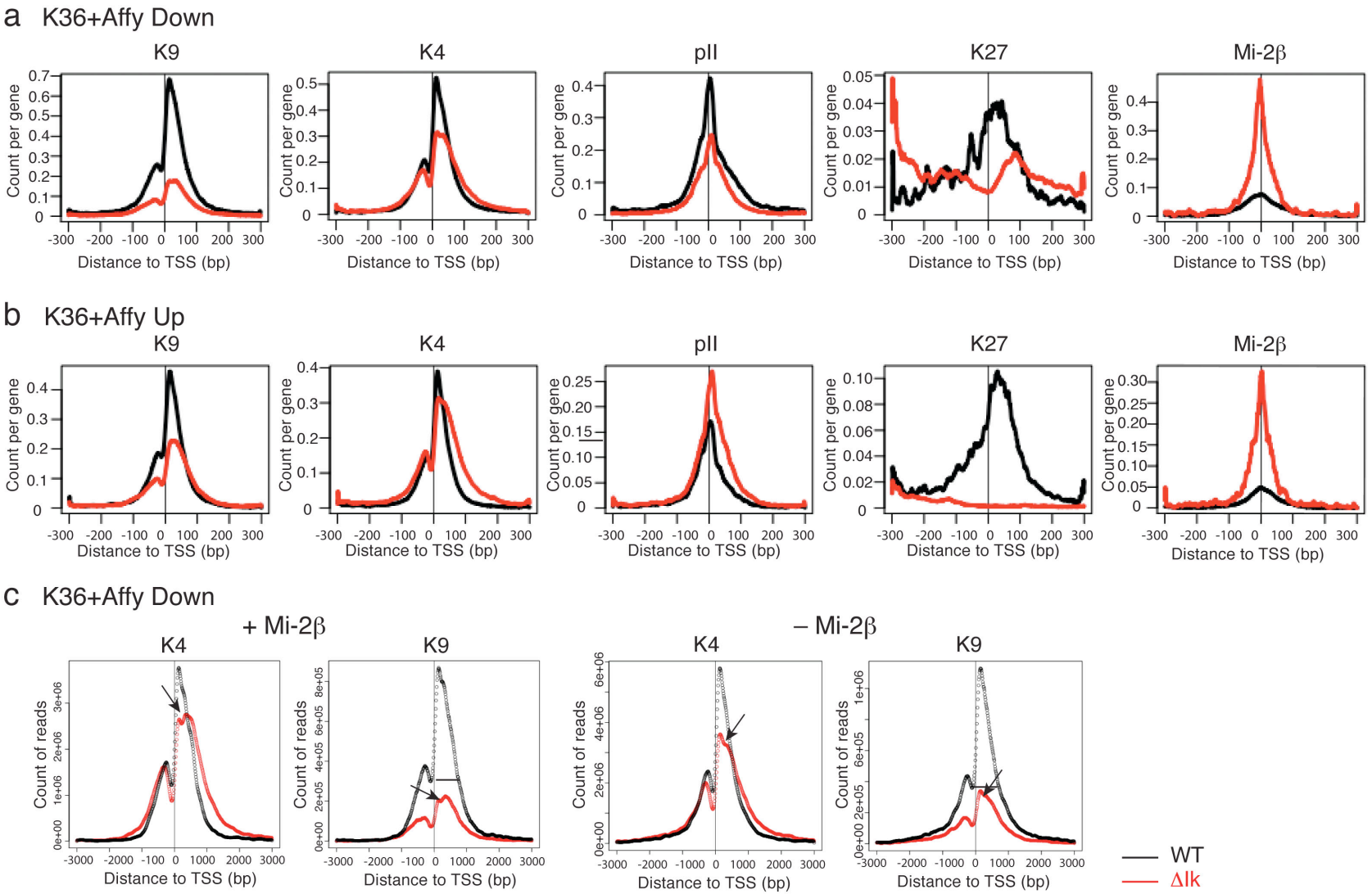

Supplementary Figure 6

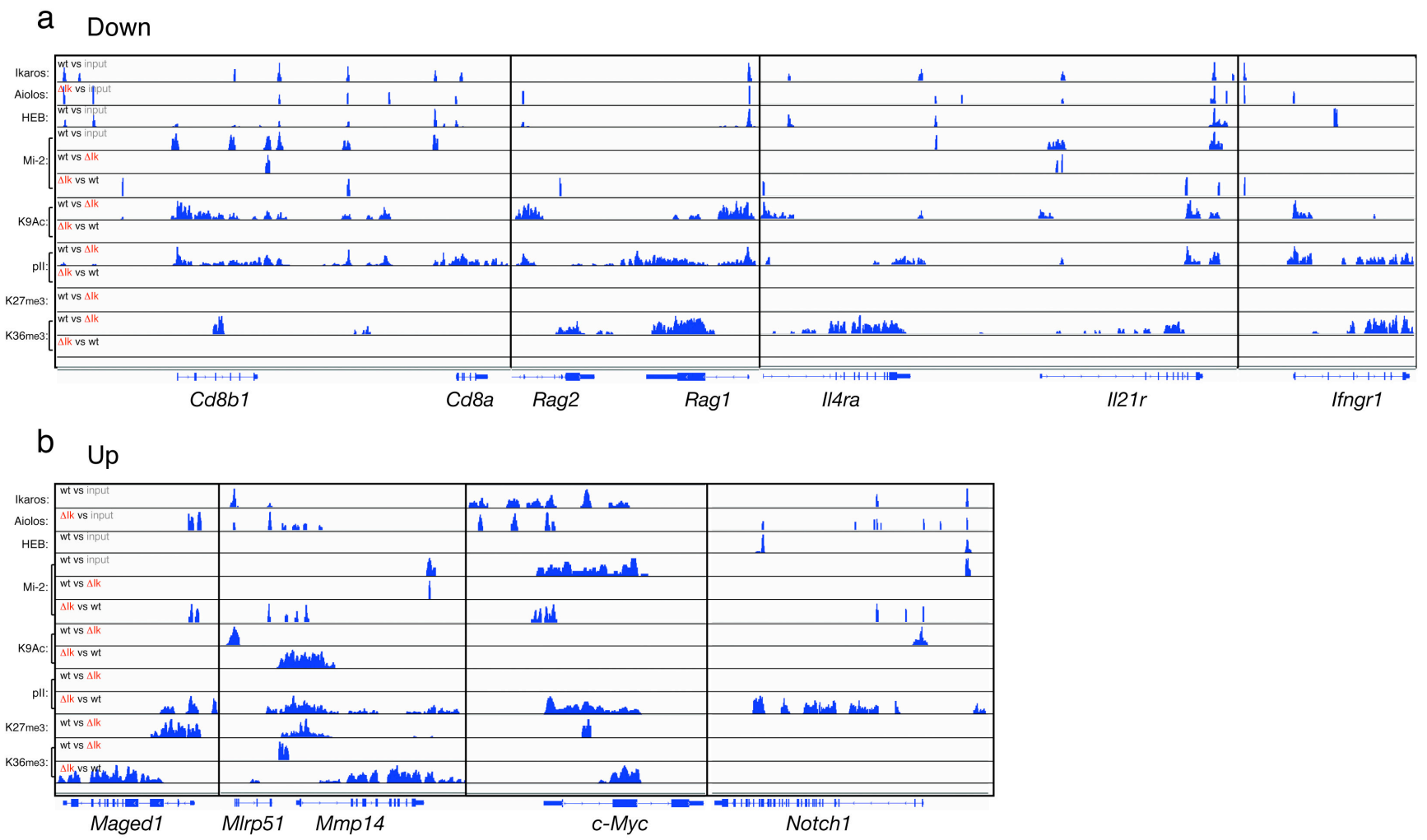

Supplementary Figure 7

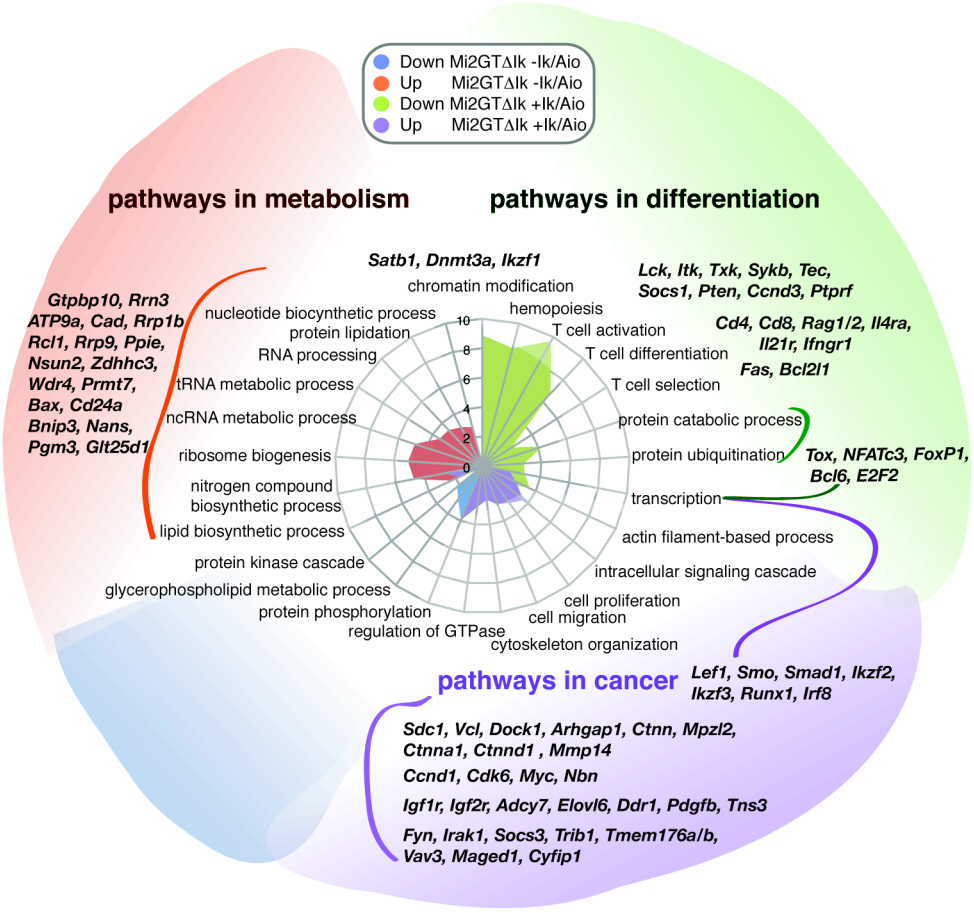

Supplementary Figure 8

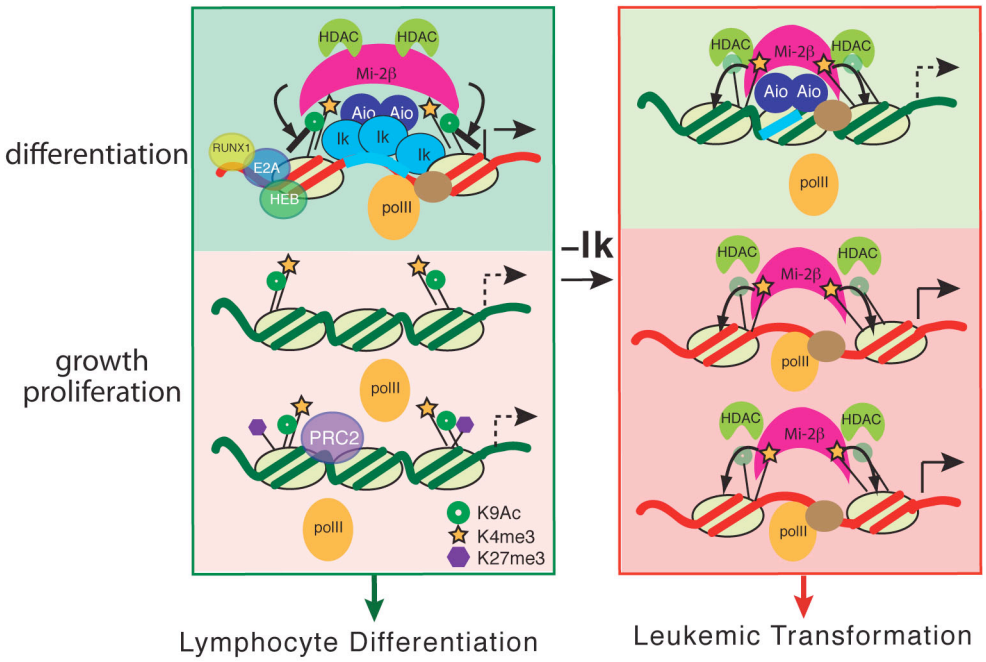

Supplementary Figure 9

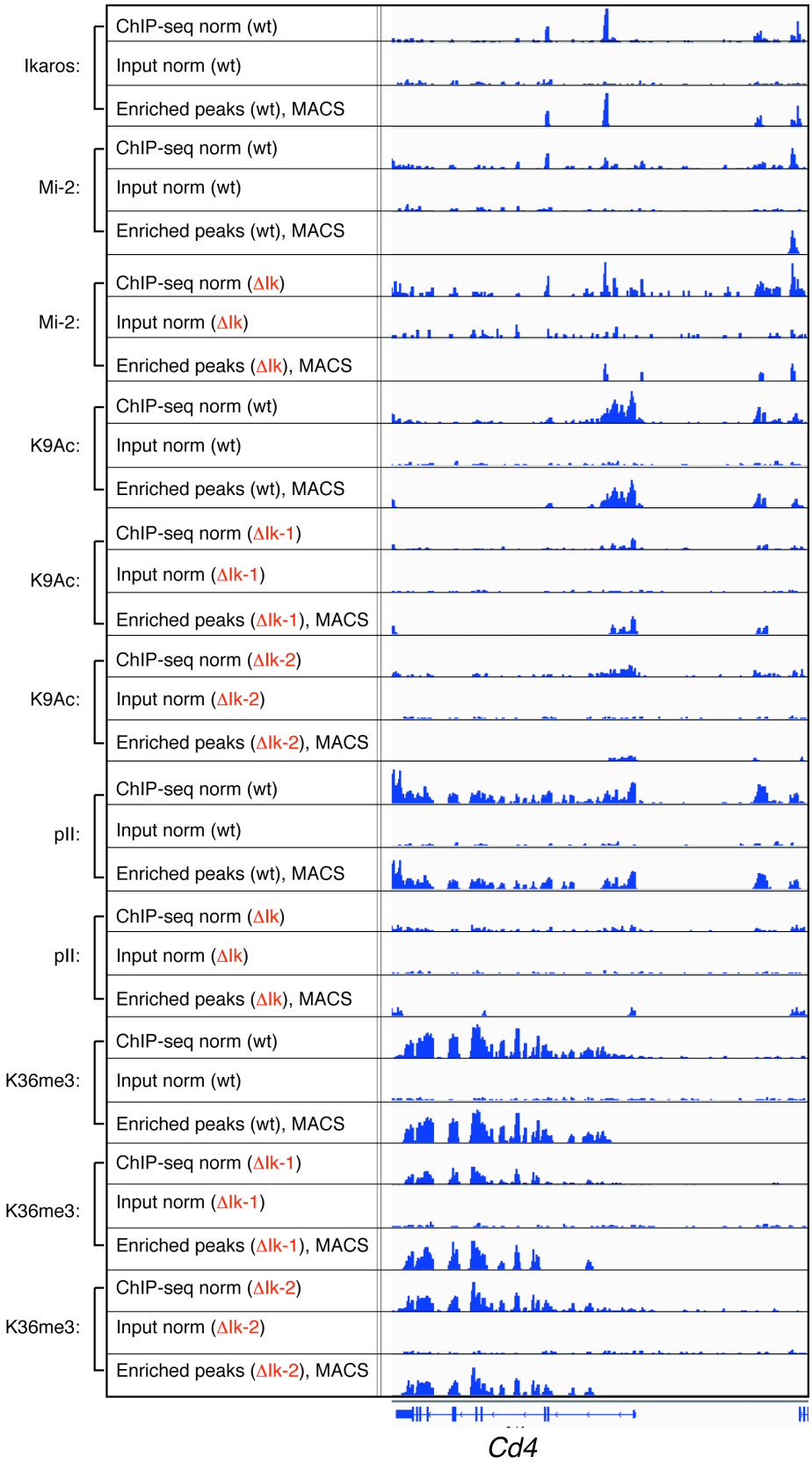

		Mi2β-flag complex		flag-Ikaros complex	
Identity	Size, kD	Mass Spec	IB	Mass Spec	IB
Mi2β	220	+	+	+	+
Mi2α	220	+	+	+	+
MTA1	75	+	ND	+	ND
MTA2	75	+	+	+	+
MTA3	75	+	+	-	+
Ikaros	66,50-48	+	+	+	+
Aiolos	66	+	+	+	+
Helios	66	-	+	+	+
p66	66	+	ND	+	ND
HDAC1	66,60	+	+	+	+
HDAC2	60	+	+	+	+
RbAp46	50	+	+	+	+
RbAp48	50	+	+	+	ND
MBD2	33, 50	+	+	ND	ND
MBD3	34	-	+	ND	ND
SMC3	150	+	+	ND	+
SMC1	150	ND	+	ND	+
SCC1	120	ND	+	ND	+
SCC3	155	ND	+	ND	+

Supplementary Table 1.

Change in H3	Ikaros GT WT	Mi-2β GT ΔIk	Aiolos GT ΔIk
H3K9Ac down in ΔIk 6807	**37%**	**67%**	**47%**
H3K9Ac up in ΔIk 1912	29%	53%	42%
RNA pII down in ΔIk 1990	**50%**	**70%**	**55%**
RNA pII up in ΔIk 1345	34%	60%	45%
H3K36me3 down in ΔIk 2408	43%	66%	50%
H3K36me3 up in ΔIk 2779	34%	58%	45%

Supplementary Table 2.

K36 and mRNA	H3K9Ac down	H3K9Ac up	H3K27 down	H3K27 up	Ik or Aio or Mi-2β
down in ΔIk 2193	64%	3%	13%	15%	64%
up in ΔIk 1760	29%	6%	33%	6%	62%

Supplementary Table 3.